

Expecting the Expected: 1 g Peak Motions in the İstanbul Metropolitan Area

E. Kalkan

4728 Donnie Lyn Way, Carmichael, CA, USA

P. Gülkan

Çankaya University, Ankara, Turkey



SUMMARY:

Using a deterministic approach, peak values of expected ground-motions are estimated for the Sea of Marmara (Turkey) region that encompasses İstanbul based on six plausible earthquake scenarios. These scenarios consist of individual and multiple rupturing of the submarine fault segments along the western part of the North Anatolian Fault Zone (NAFZ) extending into the Sea of Marmara. To quantify the regional exposure on a set of hazard maps, a total of six ground motion prediction equations (GMPEs) have been used in a combinatorial approach to account for epistemic uncertainty. In lieu of subjectively weighting the expressions, the GMPEs were weighted proportional to their relative performance in predicting the measured peak ground motions of the 1999 M7.4 Kocaeli earthquake when it ruptured the İzmit segment of the NAFZ up to the eastern reaches of İstanbul. This computational approach has resulted in consistent but different weights for each GMPE at different spectral periods. The resultant high-resolution (0.002° by 0.002° , approx. 250 m by 250 m) deterministic seismic hazard maps, that incorporate site amplification due to softer sediments, provide peak horizontal ground acceleration (PGA) and spectral acceleration values at 0.2, 0.3, 0.5, 1, 1.5, 2, 3 and 4 seconds. The median spectral acceleration at 0.3 s computed is close to 1 g along the shoreline to the west of the İstanbul metropolitan area, and 0.3 g near the financial district from all scenarios.

Keywords: Deterministic Seismic Hazard Analysis, İstanbul Metropolis, Seismic Design, Site Amplification

1. INTRODUCTION

With a population of over 13 million, İstanbul, the largest city of Turkey, is located close to one of the most tectonically active regions in Eurasia. The city was exposed to at least five damaging earthquakes (1509 Ms7.2, 1719 Ms7.4, 1766 Ms7.1, 1894 Ms7.3, 1912 Ms7.3; Ms = surface magnitude) in the last five centuries (Kalkan et al. 2009). In the last century, this region experienced a high seismic activity with seven strong events having $M \geq 7$ (M = moment magnitude) (Fig. 1). Devastating 1999 Kocaeli (M7.4) and Düzce (M7.2) earthquakes occurring on the North Anatolian Fault Zone (NAFZ) on the south of the eastern border of İstanbul province are the most recent manifestation of this high seismic activity. The 1,200 km long NAFZ has a transform mechanism, and runs across northern Turkey accommodating a ~ 25 mm/year right-lateral slip between Anatolia and the stable Eurasian plates (Straub et al. 1997; McClusky et al. 2000). Since 1939, this fault system has produced 10 $M \geq 6.7$ earthquakes in a westward-propagating sequence (Fig. 2). The exception is the 1999 earthquake in Düzce that occurred three months after the Kocaeli earthquake and 1992 Erzincan earthquake. Based on the stress transfer postulate for successively rupturing fault segments, and supported by the city's string of destructive historic earthquakes, İstanbul is considered likely to experience a major earthquake during the next few decades (Parsons 2004).

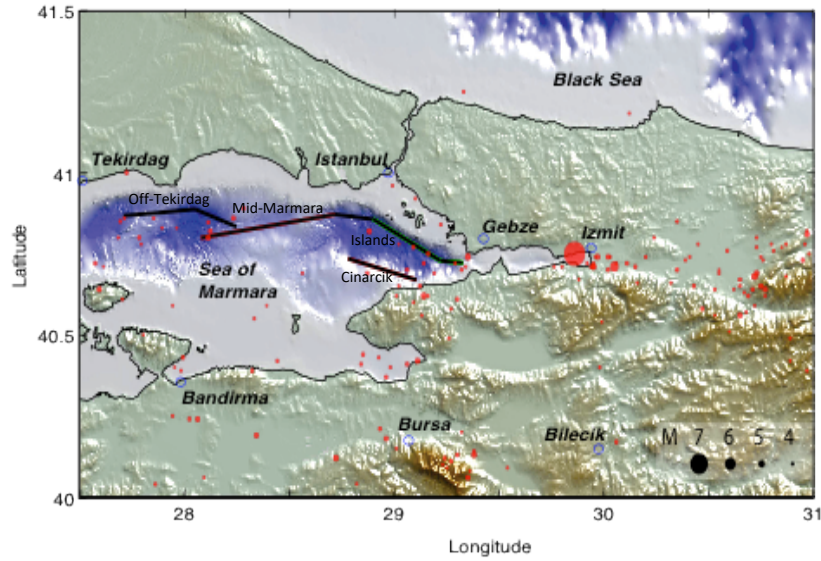


Figure 1. Map of Sea of Marmara (Turkey) region showing instrumental seismicity for the time period 1973–2010. The earthquake magnitudes are indicated by the size of the circles. Also shown are the submarine fault segments (Off-Tekirdağ, Mid-Marmara, Islands, and Çınarcık) under the Sea of Marmara floor; these fault segments may nucleate an $M \geq 6.9$ event that may strongly shake the İstanbul metropolitan Area. Nearest fault segments lie within 10 to 15 km offshore from the city's southern coastline

As far as is known, the seismic hazard for İstanbul metropolitan area is mostly due to submarine fault system at the western extension of NAFZ located south and southeast of İstanbul (Islands and Çınarcık fault segments) and southwest of the city (Mid-Marmara and Off-Tekirdağ fault segments) as shown in Figure 1 (Le Pichon et al., 2001; Armijo et al., 2002; Le Pichon et al., 2003; Armijo et al., 2005). This fault system has been recognized to have the potential to nucleate an $M \geq 7$ event, which will strongly shake the İstanbul metropolis and its surroundings. Compelled by the level of seismic risk and as a result of increased awareness of the earthquake threat, a critical assessment of the regional seismic hazard is of paramount importance to facilitate and support a wide range of earthquake engineering applications (Griffiths et al. 2007, Kalkan et al. 2009, Ozcep et al. 2010).

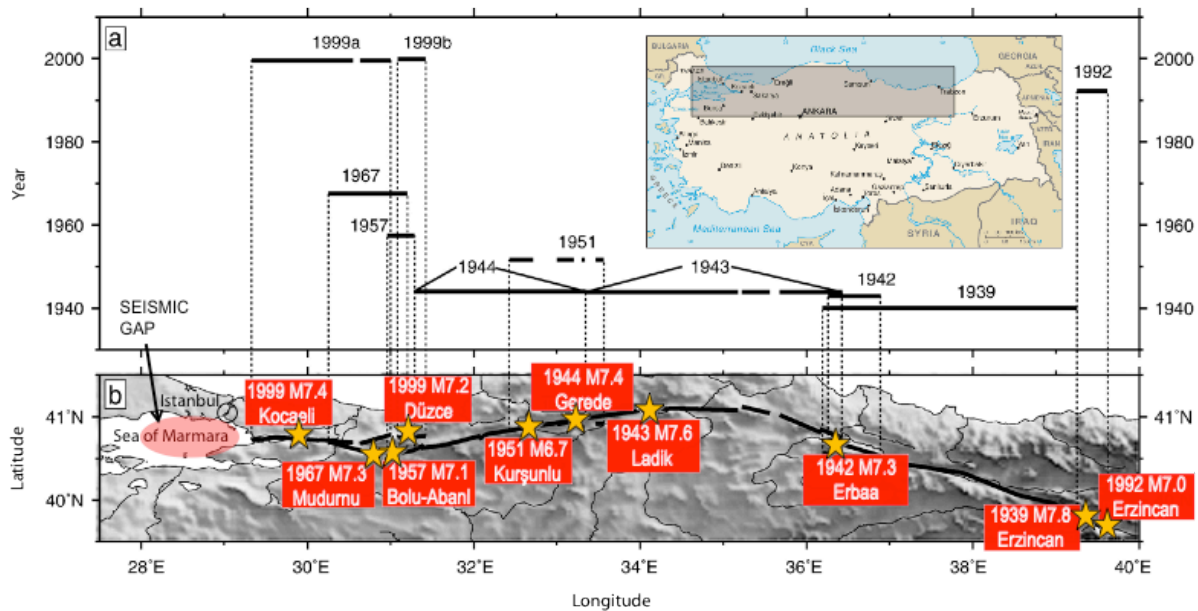


Figure 2. Sequence of westerly propagating ten large ($M \geq 6.7$) earthquakes on the North Anatolian Fault Zone (NAFZ), shown with thick black line. Potential seismic gap in the Sea of Marmara is highlighted; also shown are the fault rupture length for each event along the NAFZ; the most recent events of this sequence are the 1999 M7.4 Kocaeli (Izmit) and M7.2 Duzce earthquakes.

Both probabilistic and deterministic methods can be used to assess the seismic hazard. The probabilistic seismic hazard analysis (PSHA) maps and related products are useful in assessing risks. PSHA maps may include finer definition of seismic hazard for building codes, earthquake insurance and specific seismic design for critical infrastructure. Earlier PSHA studies for the Sea of Marmara region that encloses İstanbul are based on broadly described submarine faults and imported ground motion prediction equations (GMPEs) from the 1990s (Atakan et al. 2002; Erdik et al. 2004). Recently, seismic hazard of the region have been re-assessed in a probabilistic framework by Kalkan et al. (2009) following the general methodology developed for the U.S. national seismic hazard maps (Petersen et al. 2008) and its implementation for California (Kalkan et al. 2010). The new PSHA maps developed are based on the latest generation of global and locally derived GMPEs, and on the most current information on regional faults, and historical and instrumental seismicity data.

As opposed to the probabilistic formulation, the deterministic seismic hazard analysis is best designated as the ‘scenario’ method, and provides a clear and easily tracked way of computing seismic hazard. Scenario ground-motions are estimated motions expected from a subset of the possible earthquakes, some of which may represent just one event. For the Sea of Marmara region, scenario earthquakes and associated peak values of expected ground-motions have been estimated previously using hybrid ground motion simulations (e.g., Pulido et al. 2004). In this study peak values of expected ground-motion will be estimated using a deterministic approach where a suite of six local and global ground-motion prediction equations (GMPEs) have been used in a combinatorial approach to account for epistemic uncertainty. Six plausible earthquake scenarios have been defined for this purpose. These scenarios consist of single and multiple ruptures occurring on the Islands, Mid-Marmara, Çınarcık and Off-Tekirdağ fault segments along the western extension of the NAFZ beneath the Sea of Marmara Sea (Fig 1). Instead of subjectively weighting the GMPEs, the expressions were weighted according to their relative accuracy in predicting the measured peak ground-motions of the 1999 M7.4 Kocaeli earthquake that occurred on the İzmit segment of the NAFZ beyond the eastern border of İstanbul province. This hindsight-based computation has resulted in consistent but different weights for each GMPE that vary for different spectral periods. Seismic hazards of Sea of Marmara region are computed and projected on a set of deterministic hazard maps having a high resolution (0.002° by 0.002° , i.e., approx. 250 m by 250 m). These hazard maps incorporating the site effects were computed for peak horizontal ground acceleration (PGA) and spectral acceleration (SA) at 0.2, 0.3, 0.5, 1, 1.5, 2, 3 and 4 s for 5-percent damping. The 0.2 and 1 s periods are often used as corner spectral periods to construct a smooth design spectrum for structural design. An appropriate procedure to obtain a smooth design spectrum from a hazard spectrum is given in the ASCE/SEI 41-6 guidelines (ASCE, 2007).

2. REGIONAL SEISMOTECTONICS

Seismic reflection surveys (Smith et al. 1995; Parke et al. 2000) have revealed a complex and heterogeneous subterranean fault system as the western extension of the NAFZ under the Sea of Marmara floor. In the east at the junction of the Marmara Sea, the NAFZ is predominantly controlled by right-lateral strike-slip faults, while the plate boundary changes into a trans-tensional system that has opened a deep-basin below the Marmara Sea (Okay et al. 2000) (see Fig. 1). There is no evidence of a single, continuous, purely strike-slip fault under the sea, but a complex of segmented faults with large normal components. Although there is detailed information about the geometry of these fault segments at depths less than 5 km, due to major uncertainty concerning their deeper parts, we have assumed that these fault segments dip vertically.

In the recent past, a series of strong earthquakes have ruptured the NAFZ in this region. Kocaeli and Düzce were the latest events in a westward-propagating earthquake sequence that began with the M7.9 Erzincan earthquake in 1939 on this fault zone (Fig. 2). When the 1912 event that occurred in the west of the Sea of Marmara is taken into account (Kalkan et al. 2009), a seismic gap that has not ruptured for more than 200 years is identified (see highlighted zone in Sea of Marmara in Fig. 2). This crosses close to the northern shoreline of the Marmara Sea (Barka 1992; Stein et al. 1997), and points toward

the Mid-Marmara and Islands fault segments (Fig. 1). This seismic gap is around 150-160 km long and may generate an $M > 7$ earthquake (Hubert-Ferrari et al. 2000). Coulomb stress calculations show that shear stress has increased on the fault segments below the Sea of Marmara in the aftermath of the 1999 Kocaeli earthquake, indicating their likely impact on the rupture potential (Parsons et al. 2000).

3. SITE EFFECTS

In order to incorporate site effects (amplification due to local geological conditions) and their spatial variability on ground motion estimates, a map with the grid of Vs30 is needed (Fig. 3). This proxy map of Vs30 was determined from topographic slope calculated from a 1-km grid using the method of Wald and Allen (2007). For the Sea of Marmara region, surface soils generally have Vs30 values between 400 and 760 m/s (stiff soil to hard rock) along the southern coastal line of the Sea of Marmara. The Vs30 ranges between 200 and 400 m/s along its northern coastline that bounds the metropolitan area. Sound bedrock is located in the northeastern and eastern parts of the İstanbul metropolitan area (Ündül and Tuğrul, 2006). Softer sediments with $Vs30 < 300$ m/s are located in the southwestern parts of its European side, where a higher portion of the city's population resides. This region is prone to locally amplify ground-shaking hazard; the amplification can be as high as 2.5 times as compared to the nearby rock sites (Kalkan et al. 2012).

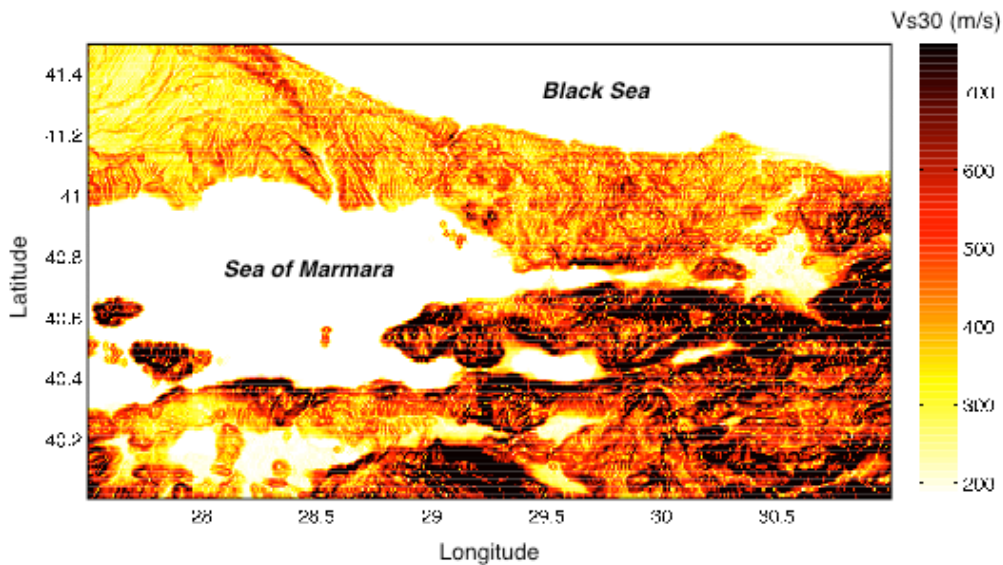


Figure 3. Map of Sea of Marmara (Turkey) region showing a proxy for the shear-wave velocity averaged over the top 30 m of the ground ($Vs30$) derived from topographic slope. Dark color = rock site, light color = soft soil site, white color = water. Most of the population in the İstanbul metropolitan area resides on soft-soil deposits, prone to amplified ground shaking during earthquakes ($Vs30$ data is taken from the USGS Global $Vs30$ Map Server: <http://earthquake.usgs.gov/hazards/apps/vs30/>).

4. SCENARIO EARTHQUAKES

Six plausible earthquake scenarios were defined for the greater İstanbul metropolitan area considering individual and multiple ruptures of the Islands, Mid-Marmara, Çınarcık, and Off-Tekirdağ fault segments. These scenarios are shown in Figure 4, where the rupture length and expected magnitudes (M_{max}) computed according to the historic seismicity and the empirical formula of Wells and Coppersmith (1994) are marked. In these scenarios, selected fault segments are assumed to rupture in strike-slip mechanism along their entire length. Hypocenter location of earthquakes is not taken as a variable because the GMPEs selected utilize a specific distance definition either as the closest distance to the co-seismic rupture plane (R_{rup}) or as the closest distance to the surface projection of the causative fault (R_{jb}); both distance measures are independent of the hypocenter location but they are depend on the fault geometry.

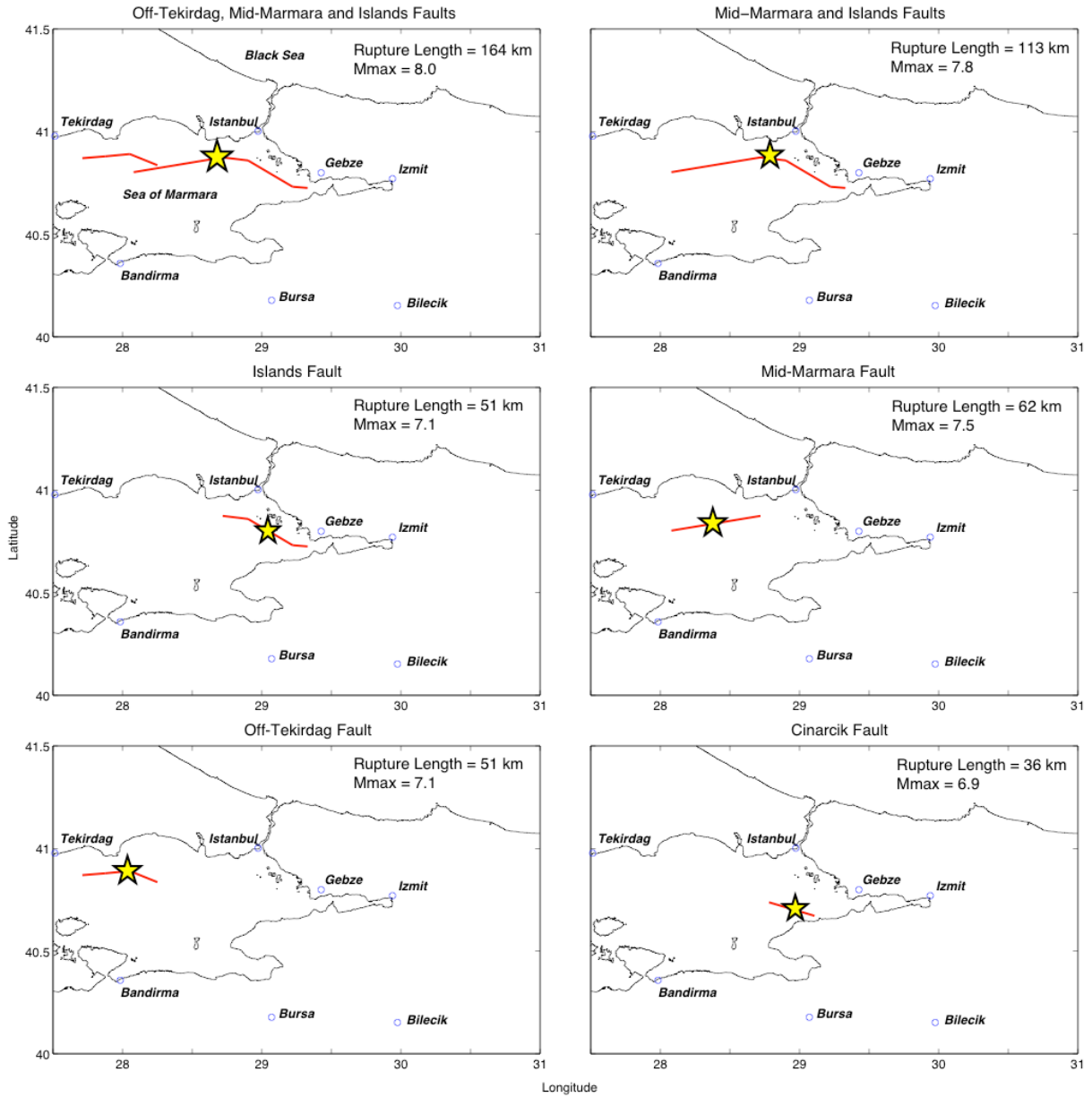


Figure 4. Six plausible earthquake scenarios defined for the greater İstanbul metropolitan area considering the individual and multiple rupturing of the Islands, Mid-Marmara, Çınarcık and Off-Tekirdağ fault segments. For each scenario, rupture length and expected magnitudes (M_{max}) computed according to the historic seismicity and Wells and Coppersmith (1994) empirical equation are shown.

In this study, only the scenario earthquakes shown above are defined because they are the source of the strongest shaking level expected for İstanbul. Our scenario earthquakes involving the combined rupture of the Islands, Mid-Marmara and Off-Tekirdağ fault segments are plausible because it has been observed that the NAFZ is continuous beneath the Sea of Marmara (Okay et al. 2000; Le Pichon et al. 2001), so it has no significant fault offsets that could stop a fault rupture. It could be argued that the significant bend between the Islands and Mid-Marmara, and between the Mid-Marmara and Off-Tekirdağ could be enough to stop a fault rupture. However, recent dynamic models of faulting have shown that even large fault bends cannot always arrest a fault rupture (Poliakov et al. 2002; Kame et al. 2003). The recent Kocaeli earthquake indeed provided a good example of a fault rupture running across a significant fault bend (Harris et al. 2002; Pulido et al. 2004).

5. GENERAL METHODOLOGY FOR HAZARD COMPUTATION

Deterministic Seismic Hazard Analysis (DSHA) uses geology and seismicity to identify earthquake sources and to interpret the largest earthquake each source is capable of producing under the presently known or hypothetical tectonic activity regardless of recurrence period. This is called Maximum Credible Earthquake (MCE), which will cause the most severe consequences at site of interest. To estimate the MCE, we considered historical seismicity and Wells and Coppersmith (1994) relation between the fault lengths versus earthquake magnitudes. Using these details and a suite of appropriate GMPEs weighted within a consistent logic tree approach, the PGA and spectral acceleration values at 0.2, 0.3, 0.5, 1, 1.5, 2, 3 and 4 seconds were estimated.

5.1. Ground-Motion Estimation

A total of six global and locally generated GMPEs were used in order to account for epistemic uncertainty. The imported GMPEs are selected from the Next Generation of Attenuation (NGA) project. They are the equations by Abrahamson and Silva (2008), Boore and Atkinson (2008), Campbell and Bozorgnia (2008), and Chiou and Youngs (2008). These GMPEs are found to be applicable for Europe and the Middle East (Stafford et al. 2008). Graizer and Kalkan (2007 and 2009) model, derived based on the NGA project database, which has some Turkish strong-motion records, is also included. Comparisons of ground motion data from a recent Turkish earthquake with the prediction of the Graizer and Kalkan model shows that this GMPE estimates the local ground motions as good as other NGA models (Akkar et al. 2011). These global GMPEs are abbreviated respectively as AS08, BA08, CB08, CY08, and GK07. The GMPE that is based on local records is by Kalkan and Gülkan (2004), and it is abbreviated as KG04.

5.2. Logic Tree Weighting

Logic tree is used to account for epistemic uncertainty in hazard analysis. Instead of subjectively weighting the GMPEs to be used for logic tree, the expressions were weighted according to the relative accuracy of their performance in predicting the observed peak motions of the 1999 M7.4 Kocaeli earthquake when it ruptured the İzmit segment of the NAFZ up to the eastern reaches of İstanbul (see Fig. 2). In this approach, a GMPE providing a smaller overall standard deviation of prediction among other GMPEs is weighted more. The relative weights of GMPEs for each intensity measure (IM) (that is, PGA or spectral accelerations at selected periods) is calculated using a residual analysis as follows:

- 1) Compute the residuals for the i^{th} GMPE; residuals correspond to the difference between the observations and predictions in natural-log space,
- 2) Compute standard deviation of residuals, σ_i for the i^{th} GMPE,
- 3) Relative weight, W_i , for the i^{th} GMPE is computed as $W_i = \left[1 / \sigma_i^2 \right] / \left[\sum_{i=1,n} (1 / \sigma_i^2) \right]$, where n is

the total number of GMPEs selected and $\sum_{i=1,n} W_i = 1$.

This de-facto segregation has resulted in consistent but different weights for each GMPE varying at different spectral periods as shown in Figure 5. The local GMPE, the KG04, performs best at PGA and spectral acceleration at 0.2, 0.3, 0.5, 1 and 1.5 s; the predictions of this GMPE are limited to 2 s. For longer periods (i.e., 3 and 4 s), the remaining five global GMPEs were used; among them the largest weight is computed for the AS08 due to its better accuracy in predicting the measured peak ground motions of the Kocaeli earthquake as compared to other GMPEs.

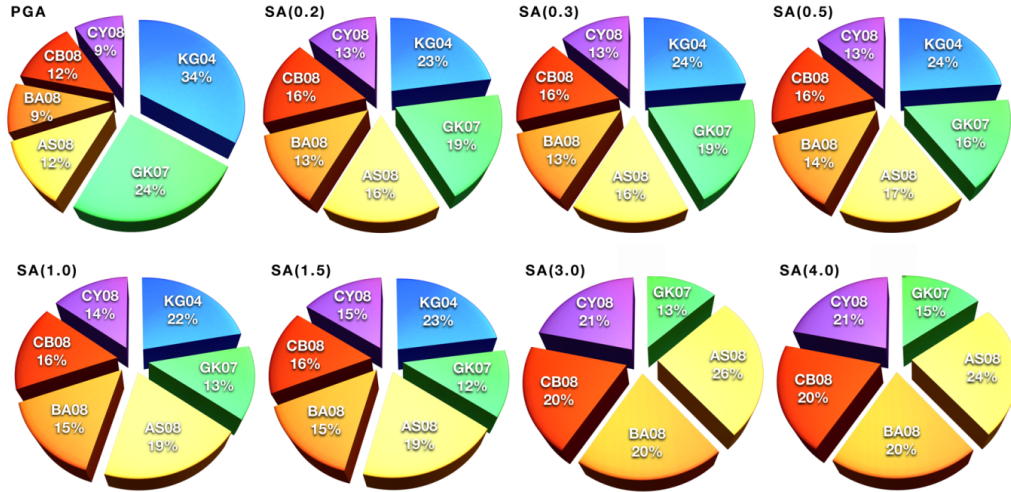


Figure 5. Logic tree weights of GMPEs computed according to their relative performances in predicting the peak motions of the 1994 M7.4 Kocaeli earthquake for PGA and spectral accelerations at 0.2, 0.3, 0.5, 1, 1.5, 2, 3 and 4 seconds; [local GMPE is KG04 = Kalkan and Gulkan, 2004; and global GMPEs are GK07 = Graizer and Kalkan, 2007; AS08 = Abrahamson and Silva, 2008; BA08 = Boore and Atkinson, 2008; CB08 = Campbell and Bozorgnia, 2008; CY08 = Chiou and Youngs, 2008].

6. SEISMIC HAZARD RESULTS

For each earthquake scenario, the following set of maps (with a resolution of 0.002° by 0.002°, or approx. 250 m by 250 m) were generated:

- Median value of peak horizontal ground acceleration (PGA),
- Median value of spectral accelerations at 0.2, 0.3, 0.5, 1, 1.5, 2, 3 and 4 seconds for 5%-damping,
- Ratio comparing shaking level of the 1999 M7.4 Kocaeli event with those in the scenarios for PGA and spectral accelerations,
- Spectral amplification.

For brevity, Figure 6 shows only the median values of PGA. This map incorporates site effects by assigning a V_{s30} value corresponding to each grid point by using the map in Figure 3 as a proxy. The distribution of PGA values, shown by the color gradient, indicates higher shaking level along the coastline of İstanbul, where Off-Tekirdağ, Mid-Marmara and Islands faults are about 10-15 km offshore. Multiple rupturing of these fault segments is expected to shake the coastal districts of the city in the European side (these are Avcılar, Bahçeşehir, Bakırköy and Beylikdüzü) with a PGA of 0.5 – 0.7 g. Intense PGA levels are also expected at the İstanbul Strait where it opens to the Sea of Marmara. The level of shaking gradually diminishes toward the north. The median PGA ranges between 0.4 g and 0.6 g at the coastal districts of the city in the Asian side (these are Kadıköy, Maltepe, Kartal, Pendik and Tuzla). The estimated PGA increases to as much as 0.65 g at Adalar district (Marmara Islands). Table 1 lists the PGA and spectral acceleration (SA) values at 0.2, 0.3, 0.5, 1, 1.5, 2, 3 and 4 s computed at central point of each district of the İstanbul metropolitan area considering the worst-case earthquake scenario (that is, multiple rupturing of Off-Tekirdağ, Mid-Marmara and Islands fault segments). In this table, the districts expected to experience the highest shaking are also highlighted. This table shows that the largest expected spectral acceleration at short periods (0.3 s) that are close to the fundamental vibration period of 3- and 4-story reinforced concrete buildings is close to 1 g along the shoreline to the west of İstanbul, and at Sea of Marmara islands. The majority of the building stock in these parts of the city

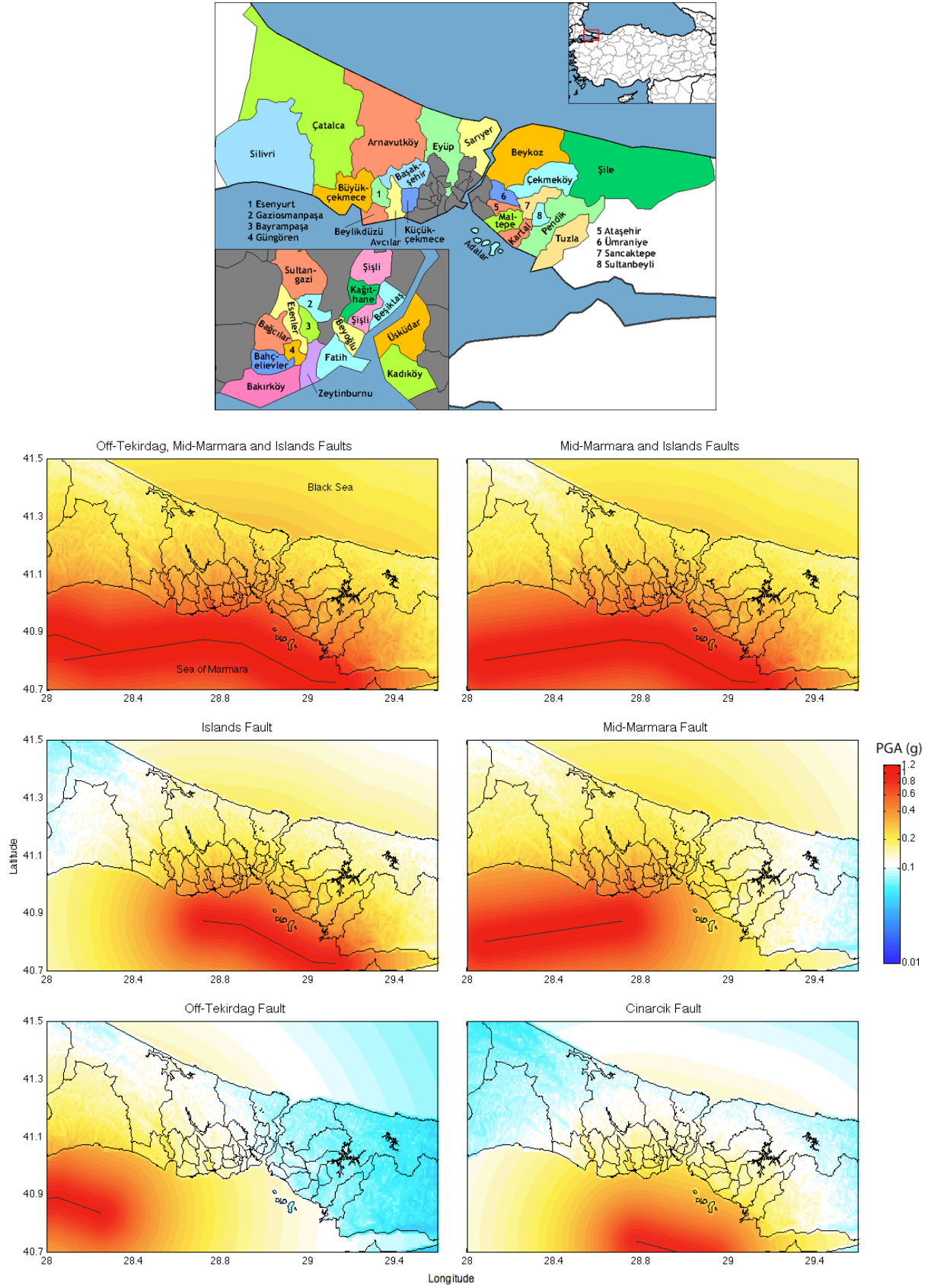


Figure 6. Peak ground acceleration (PGA) maps for the İstanbul metropolitan area considering six earthquake scenarios. Median computed PGA is 0.65 g along the shoreline to the west of İstanbul (Bakırköy district) and at Marmara Islands (Adalar district) as a result of multiple rupturing of Off-Tekirdağ, Mid-Marmara and Islands faults; map (top panel) shows districts of the İstanbul metropolitan Area.

Table 1. Peak ground acceleration (PGA) and spectral acceleration (SA) values (at 0.2, 0.3, 0.5, 1, 1.5, 2, 3 and 4 s for 5%-damping) computed at central point of districts in the İstanbul metropolitan area considering the worst-case earthquake scenario (that is, multiple rupturing of Off-Tekirdağ, Mid-Marmara and Islands fault segments). The districts, expected to experience the highest shaking, are highlighted.

District Name	Population	Area (km ²)	Population Density (people/km ²)	PGA (g)	Spectral Accelerations							
					(0.2 s)	(0.3 s)	(0.5 s)	(1 s)	(1.5 s)	(2 s)	(3 s)	(4 s)
Adalar	10,460	11.05	947	0.65	0.91	0.95	0.71	0.59	0.37	0.28	0.20	0.15
Arnavutköy	148,419	506.5	293	0.27	0.36	0.37	0.27	0.24	0.16	0.12	0.09	0.07
Ataşehir	345,588	25.87	13,359	0.42	0.57	0.57	0.41	0.36	0.23	0.17	0.13	0.10
Avcılar	322,190	41.92	7,686	0.55	0.77	0.78	0.57	0.48	0.29	0.22	0.16	0.12
Bağcılar	719,267	22.4	32,110	0.38	0.53	0.53	0.39	0.33	0.21	0.15	0.11	0.08
Bahçelievler	571,711	16.57	34,503	0.56	0.74	0.77	0.55	0.48	0.32	0.24	0.19	0.14
Bakırköy	214,821	29.65	7,245	0.65	0.87	0.90	0.65	0.56	0.37	0.28	0.21	0.16
Başakşehir	193,750	104.5	1,854	0.37	0.50	0.51	0.37	0.32	0.21	0.15	0.11	0.08
Bayrampaşa	272,196	9.5	28,652	0.41	0.56	0.56	0.41	0.36	0.23	0.17	0.13	0.10
Beşiktaş	191,513	18.04	10,616	0.34	0.47	0.48	0.35	0.30	0.20	0.15	0.11	0.08
Beykoz	241,833	310.4	779	0.23	0.32	0.32	0.24	0.21	0.13	0.10	0.07	0.05
Beylikdüzü	186,847	37.74	4,951	0.52	0.72	0.73	0.53	0.45	0.28	0.20	0.15	0.11
Beyoğlu	247,256	8.96	27,596	0.49	0.68	0.69	0.50	0.42	0.26	0.19	0.14	0.10
Büyüçekmece	151,954	157.7	964	0.45	0.62	0.63	0.46	0.40	0.26	0.19	0.15	0.11
Çatalca	61,566	1040	59	0.25	0.35	0.35	0.26	0.22	0.14	0.10	0.07	0.05
Çekmeköy	135,603	148	916	0.23	0.31	0.30	0.22	0.19	0.12	0.09	0.06	0.05
Esenler	468,448	18.51	25,308	0.37	0.51	0.52	0.38	0.33	0.21	0.16	0.12	0.09
Esenyurt	335,316	43.12	7,776	0.49	0.65	0.67	0.48	0.43	0.28	0.22	0.17	0.13
Eyüp	317,695	228.1	1,393	0.26	0.35	0.35	0.26	0.22	0.15	0.11	0.08	0.06
Fatih	455,498	15.93	28,594	0.50	0.67	0.68	0.49	0.44	0.29	0.22	0.17	0.13
Gaziosmanpaşa	464,109	11.67	39,769	0.34	0.47	0.48	0.35	0.30	0.19	0.14	0.10	0.08
Güngören	318,545	7.17	44,427	0.50	0.68	0.69	0.50	0.44	0.29	0.22	0.17	0.13
Kadıköy	550,801	25.07	21,971	0.46	0.63	0.64	0.46	0.41	0.27	0.20	0.16	0.12
Kağıthane	418,229	14.83	28,202	0.31	0.44	0.44	0.32	0.27	0.17	0.12	0.09	0.06
Kartal	427,156	38.54	11,083	0.52	0.70	0.72	0.52	0.45	0.29	0.22	0.17	0.12
Küçükçekmece	662,566	37.25	17,787	0.46	0.65	0.65	0.47	0.40	0.25	0.18	0.13	0.10
Maltepe	415,117	53.06	7,824	0.41	0.56	0.57	0.42	0.36	0.23	0.17	0.12	0.09
Pendik	520,486	180.2	2,888	0.43	0.61	0.61	0.44	0.37	0.23	0.17	0.12	0.09
Sancaktepe	223,755	61.87	3,617	0.26	0.36	0.36	0.27	0.23	0.15	0.11	0.08	0.06
Sarıyer	276,407	151.3	1,827	0.23	0.32	0.31	0.24	0.20	0.13	0.09	0.07	0.05
Silivri	118,304	869.5	136	0.31	0.43	0.43	0.32	0.27	0.17	0.12	0.09	0.07
Sultanbeyli	272,758	28.86	9,451	0.33	0.46	0.46	0.34	0.29	0.18	0.13	0.10	0.07
Sultangazi	436,935	36.24	12,057	0.34	0.46	0.47	0.34	0.30	0.20	0.16	0.12	0.09
Şile	25,169	781.7	32	0.18	0.24	0.24	0.18	0.16	0.11	0.08	0.06	0.04
Şişli	314,684	34.98	8,996	0.42	0.56	0.58	0.42	0.37	0.25	0.19	0.16	0.12
Tuzla	165,239	123.9	1,334	0.57	0.78	0.80	0.58	0.50	0.31	0.24	0.18	0.13
Ümraniye	553,352	45.3	12,215	0.40	0.54	0.55	0.40	0.36	0.24	0.19	0.15	0.11
Üsküdar	529,550	35.34	14,984	0.34	0.48	0.48	0.35	0.30	0.19	0.14	0.10	0.07
Zeytinburnu	288,743	11.31	25,530	0.53	0.73	0.74	0.54	0.46	0.30	0.22	0.17	0.13

including those at Avcılar, Bakırköy, Bahçeşehir and Adalar districts are 3-5 story heights, which are the most vulnerable. At the city's financial district (Sarıyer), which has mostly mid- and high-rise buildings (5- to 30-story), the largest expected spectral acceleration at 0.5, 1 and 3 s are 0.24, 0.2 and 0.07 g, respectively. This level of shaking indicates that the financial district of the city will be shaken in much less intensity than its shoreline.

7. SUMMARY

Sea of Marmara (Turkey) region that encompasses İstanbul, one of the largest Euro-Asian metropolises, is under the threat of a major earthquake. While much geological discussion has been recorded on identifying the characteristics of the faults, relatively little has been done for translating that background to engineering design tools. In order to provide a scientific basis for seismic design applications, this paper presents a deterministic assessment of the seismic hazard for the region focussing on the İstanbul metropolitan area. The expected intensity of ground shaking was determined for six plausible earthquake scenarios defined by examining geologic, tectonic, historic and instrumental evidence. These scenarios consist of individual and multiple rupturing of the submarine fault segments of the North Anatolian Fault Zone (NAFZ) extending under the Sea of Marmara floor. A total of six global and regional ground motion prediction equations (GMPs) have been used in a combinatorial approach to delineate the regional seismic hazard on a suite of hazard maps at different

spectral periods. The principal differences of the study described here and the previous studies that have focused on the İstanbul Metropolitan (e.g., Atakan et al. 2002; Erdik et al. 2004) are the following:

1. Instead of a subjective selection, logic-tree weights of GMPEs were determined here according to their relative performances in predicting observed ground motions of the 1999 M7.4 Kocaeli earthquake. This non-subjective computational approach led to each GMPE having varying logic tree weights at each spectral period [that is, PGA or SA(T), where $T = 0.2$ through 4 s]. This analytical approach resulted in larger weight for the GMPE of Kalkan and Gülkan (2004) developed from indigenous sources as compared to other global GMPEs based on the Next Generation of Attenuation (NGA) project database.
2. For the hazards maps, we have incorporated the potential site amplification by the near-surface soils (using a V_{s30} as a proxy) to develop a more complete depiction of potential seismic shaking hazards throughout the Sea of Marmara region.
3. The seismic hazard maps were computed on a grid of approx. 250 m by 250 m – a very fine resolution.
4. The characteristics attributed to the seismogenic sources and use of NGA relations in addition to a local GMPE are also major improvements.

A set of deterministic seismic hazard maps generated here is a complement of the probabilistic seismic hazard maps previously presented in Kalkan et al. (2009). These maps are intended to shed light on future assessments of risk to structures within the İstanbul metropolitan area and, we hope, serve as a reminder to improve design and construction practices to minimize losses of life and property. Our gridded deterministic hazard results can be directly used in the design of new and evaluation of existing structures.

ACKNOWLEDGMENT

We wish to thank Art Frankel for his help with the USGS deterministic seismic hazard code. We also thank Mahmut Baş, head of the Metropolitan Municipality Soils and Earthquake Division for kindly providing us the district map of İstanbul province. Special thanks are extended to Art Frankel, Ross Stein, Charles Muller, Ayhan Irfanoglu and Ömer Emre who reviewed this paper and provided their constructive comments and suggestions, which were helpful in improving its technical quality and presentation.

REFERENCES

- Abrahamson, N. A. and W. J. Silva (2008). Summary of the Abrahamson and Silva NGA ground motion relations. *Earthquake Spectra* **24** (1), 67–98.
- Akkar, S., Aldemir, A., Askan, A., Bakır, S., Canbay, E., Demirel, O., Erberik, A., Gülerce, Z., Gülkan, P., Kalkan, E., Prakash, S., Sandıkkaya, A., Sevilgen, V., Uğurhan, B., Yenier, E., (2011). “8 March 2010 Elazığ-Kovancılar (Turkey) Earthquake: Observations on Ground Motions and Building Damage”, *Seismological Research Letters*: **82**, (1), 42-58.
- American Society of Civil Engineers (ASCE), 2007. Seismic Rehabilitation of Existing Buildings, Report No. 41-6, p 423, ISBN: 9780784408841.
- Armijo, R., B. Meyer, S. Navarro, G. King, and A. Barka (2002). Asymmetric slip partitioning in the Marmara Sea pull-apart: A clue to propagation processes of the North Anatolian fault? *Terranova* **14**, 80–86.
- Armijo, R., N. Pondard, B. Meyer, G. Üçarcus, B. Mercier de Lépinay, J. Malavieille, S. Dominguez, M.-A. Gustcher, S. Schmidt, C. Beck, N. Çağatay, Z. Cakir, C. Imren, K. Eris, B. Natalin, S. Özalaybey, L. Tolun, I. Lefèvre, L. Seeber, L. Gasperini, C. Rangin, Ö. Emre, and K. Sarikavak (2005). Submarine fault scarps in the Sea of Marmara pull-apart (North Anatolian Fault): Implications for seismic hazard in İstanbul, *Geochem. Geophys. Geosyst.* **6**(6), 1–29.
- Atakan, K., Ojeda, A., Meghraoui, M., Barka, A. A., Erdik, M. and Bodare, A. (2002). Seismic Hazard in İstanbul following the 17 August 1999 Izmit and 12 November 1999 Düzce Earthquakes, *Bull. Seism. Soc. Am.* **92**, no. 1, 466-482.
- Barka, A. (1992). The North Anatolian fault zone, *Annales Tectonicae*, **6**, 164-195.
- Boore, D. M. and Atkinson, G. (2008). Ground motion Prediction Equations for the Average Horizontal Component of PGA, PGV, and 5%-Damped PSA at Spectral Periods between 0.01 s and 10.0 s, *Earthquake Spectra*, **24**, no. 1, 99-138.
- Campbell, K. and Bozorgnia, Y. (2008). NGA Ground motion Model for the Geometric Mean Horizontal

- Component of PGA, PGV, PGD and 5% Damped Linear Elastic Response Spectra for Periods Ranging from 0.01 to 10 s, *Earthquake Spectra*, **24**, no. 1, 139-171.
- Chiou, B. and Youngs, R. (2008). An NGA Model for the Average Horizontal Component of Peak Ground motion and Response Spectra, *Earthquake Spectra*, **24**, no. 1, 173-215.
- Erdik, M., Demircioğlu, M., Şeşetyan, K., Durukal, E. and Siyahi, B. (2004). Earthquake hazard in Marmara region, Turkey, *Soil Dynamics and Earthquake Engineering*, **24**, 605-631.
- Graizer, V. and Kalkan, E. (2007). Ground motion attenuation model for peak horizontal acceleration from shallow crustal earthquakes, *Earthquake Spectra*, **23**, pp. 585–613.
- Graizer, V. Kalkan, E. (2009). “Prediction of Response Spectral Acceleration Ordinates based on PGA Attenuation”, *Earthquake Spectra*, **25**, No. 1, pp. 36 – 69.
- Griffiths, J.H.P., Irfanoglu A. and Pujol, S. Istanbul at the Threshold: An Evaluation of the Seismic Risk in Istanbul, *Earthquake Spectra*, **23**(1), 63-75.
- Harris, R., Dolan, J.F., Harleb, R., Day, S. (2002). A 3D dynamic stress transfer model of intraequake triggering. *Bull. Seismol. Soc. Am.* **92** (1), 245–255.
- Hubert-Ferrari, A. Barka, A.A. Jacquess, E. Nalbant, S.S. Meyer, B. Armijo, R. Tapponier, P. King, G.C.P. (2000). Seismic hazard in the Marmara Sea following the Izmit earthquake. *Nature*, 404, 269-272.
- Kalkan, E. and Gülkan, P. (2004). Site-dependent spectra derived from ground motion records in Turkey, *Earthquake Spectra* **20**, no. 4, 1111-1138.
- Kalkan, E., Wills, C.J. and Brannum, D.M. (2010). Seismic hazard mapping of California considering site effects. *Earthquake Spectra*, **26**:3, 1039-1055.
- Kalkan E., Gülkan P., Yılmaz N. and Çelebi M. (2009). Re-Examination of Probabilistic Seismic Hazard in the Marmara Sea Region, *Bull. Seismol. Soc. Am.*, **99**, no. 4, pp. 2127–2146.
- Kame, N., Rice, J., Dmowska, R., (2003). Effects of prestress state and rupture velocity on dynamic fault branching. *J. Geophys. Res.* **108** (B5), 2265.
- Le Pichon, X., Şengör, A.M.C., Demirbağ, E., Rangin, C., İmren, C., Armijo, R., Görür, N., Çağatay, N., Mercier de Lepinay, B., Meyer, B., Saatçılar, R. and Tok, B. (2001). The active main Marmara fault, *Earth and Planetary Science Letters* **192**, 595-616.
- Le Pichon, X., N. Chamot-Rooke, C. Rangin, and A. M. C. Sengor (2003). The North Anatolian Fault in the Marmara Sea 2003, *J. Geophys. Res. B Solid Earth Planets* **108**, 2170–2179.
- Okay, A.I., Özcan, A.K., İmren, C., Güney, A.B., Demirbağ, E. and Kuşçu İ. (2000). Active faults and evolving strike-slip basins in the Marmara Sea, northwest Turkey: a multichannel seismic reflection study, *Tectonophysics*, **321**, 189-218.
- Ozcep, F., Karabulut, S., Korkmaz, B., Zarif, H. (2010). Seismic Microzonation Studies in Sisli / Istanbul (Turkey), Scientific Research and Essay, **5**(13), 1595 –1614.
- Parke, J.R., Minshull, T.A., Anderson, G. et al. et al. (1999). Active faults in the Marmara Sea, western Turkey, imaged by seismic reflection profiles, *Terra Nova*, **11**, 223-227.
- Parsons, T. Toda, S. Stein, R. S. Barka, A. and Dieterich, J.H. (2000). Heightened odds of large earthquake near İstanbul: an interaction-based probability calculation. *Science*, **288**, 661-665.
- Parsons, T. (2004). Recalculated probability of $M \geq 7$ earthquakes beneath the Marmara Sea, Turkey, *J. Geophys. Res.*, **109**, no. B05304, 1-21.
- Poliakov, A., Rice, J., Dmowska, R. (2002). Dynamic shear rupture interactions with fault bends. *J. Geophys. Res.* **107** (B11), 2295.
- Pulido, N., Ojeda, A., Atakan, K. and Kubo, T. (2004). Strong ground motion estimation in the Marmara Sea region (Turkey) based on scenario earthquake, *Tectonophysics*, **39**, 357-374.
- Smith, A.D., Taymaz, T., Oktay, F., Yüce, H., Alpar, B., Başaran, H., Jackson, J.A., Kara, S. and Şimşek, M. (1995). High-resolution seismic profiling in the Marmara Sea (Northwest Turkey); late Quaternary sedimentation and sea-level changes, *Geological Society of America Bulletin*, **107**, 923-936.
- Stafford, P.J., Strasser, F.O. and Bommer, J.J. (2008). An evaluation of the applicability of the NGA models to ground motion prediction in the Euro-Mediterranean region. *Bulletin of Earthquake Engineering* **6**, no. 2, 149-177.
- Stein, R.S., Barka, A.A. and Dieterich, J.H. (1997). Progressive failure on North Anatolian Fault since 1939 by earthquake stress triggering. *Geophys. J. Int.*, **128**, 594-604.
- Ündül, Ö. and Tuğrul, A. (2006). The engineering geology of İstanbul, Turkey, Proceedings of IAEG 2006 Engineering Geology for tomorrow's cities, 6 – 10 September, 2006, Nottingham, England, Proceedings p 34 & Symposium CD, paper no. 392.
- Wald, D.J. and Allen, T.I. (2007). “Topographic slope as a proxy for seismic site conditions and amplification”, *Bull. Seismo. Soc. Am.*, **97**, pp. 1379 – 1395.
- Wells, D.L. and Coppersmith, K.J. (1994). New empirical relationships among magnitude, rupture length, rupture width, rupture area, and surface displacement, *Bull. Seism. Soc. Am.* **84**, no. 4, 974-1002.